Probing the longest dark matter lifetimes with the Line Emission Mapper

Gordan Krnjaic[1,2,3,*] and Elena Pinetti[1,2,†]

[1]*Fermi National Accelerator Laboratory, Theoretical Astrophysics Group, Batavia, Illinois 60510, USA*
[2]*University of Chicago, Kavli Institute for Cosmological Physics, Chicago, Illinois 60637, USA*
[3]*University of Chicago, Department of Astronomy and Astrophysics, Chicago, Illinois 60637, USA*

In the next decade, the proposed Line Emission Mapper (LEM) telescope concept is poised to revolutionize Galactic and extragalactic x-ray sensitivity. The instruments aboard LEM feature unprecedented eV scale energy resolution and an effective area of 1600 cm^2 at 0.5 keV. Such features are ideally suited to explore decaying dark matter candidates that predict X-ray signals, including axion-like particles and sterile neutrinos. We present the first forecast of LEM sensitivity to dark matter decays and find sensitivity to lifetimes beyond $\sim 10^{32}$ s in the keV range, surpassing current limits by several orders of magnitude. Notably, our results show that LEM will be the first ever instrument to probe such long dark matter lifetimes in any mass range for any decay channel.

I. INTRODUCTION

While the evidence for the existence of dark matter (DM) is overwhelming, its particle nature remains elusive (see Ref. [1] for a review). If DM particles are metastable on cosmological timescales, their visible decay products may be observed as excesses over astrophysical backgrounds with terrestrial and space-based telescopes [2,3]. This technique is particularly promising for keV scale DM particles whose decays yield x-ray lines, including well-motivated models of axionlike particles [4] and sterile neutrinos [5].

The Line Emission Mapper (LEM) is a proposed next-generation x-ray telescope consisting of two instruments aboard; an imaging calorimeter and a grazing-incidence mirror with a large effective area (1600 cm^2 at 0.5 keV) [6]. Both instruments are optimized for detecting soft x-ray emission in the 0.2–2 keV energy interval. This innovative concept includes a large angular field of view ($30' \times 30'$) with a $10''$–$15''$ angular resolution. LEM will have a remarkable grasp of 140×10^4 cm^2 arcmin^2 at 0.5 keV, nearly three orders of magnitude better than the future x-ray telescope XRISM Resolve, which is planned to be launched in late 2030s [7].

One of the most striking and distinctive features of this mission design is the exceptional spectral resolution of 1–2 eV, which will allow numerous emission lines to be detected with unparalleled precision. From a DM perspective, this energy resolution will have the potential to identify a photon line of DM origin as well as better

*krnjaicg@fnal.gov
†epinetti@fnal.gov

characterize the astrophysical background of our particle signal. This mission plan will be submitted during the NASA 2023 Astrophysics Probes call for proposals, with the goal of being launched in 2032 [6]. This timeline makes it even more important to forecast the sensitivity of this next-generation telescope to previously unexplored DM parameter space.

To estimate the order of magnitude of LEM sensitivity to the DM lifetime, consider the approximation in which DM particles of mass m decay to nearly monochromatic photons with lifetime τ in the Galaxy. For an instrument with $N_{\rm bg}$ expected background events in the energy bin containing $E_\gamma \approx m/2$, the DM lifetime τ for which the signal exceeds the 2σ statistical uncertainty satisfies,

$$\tau \sim 10^{31} \text{ s} \left(\frac{\text{keV}}{m} \right) \left(\frac{t_{\rm obs}}{10 \text{ Ms}} \right) \left(\frac{A_{\rm eff}}{10^3 \text{ cm}^2} \right) \left(\frac{\Delta\Omega}{10^{-4} \text{ sr}} \right) \sqrt{\frac{10^4}{N_{\rm bg}}},$$

where $A_{\rm eff}$ is the effective area, $t_{\rm obs}$ is the duration of the observation, and we have used Eq. (3) with $D \approx 28$, rescaled by the field of view $\Delta\Omega$ of the telescope (see below). Note that for these LEM inspired values, this lifetime reach exceeds the longest DM lifetime limits ever achieved in any channel at any DM mass; the current record is $\sim 10^{30}$ s from observations of ultrahigh-energy cosmic rays [8].

We explore the LEM sensitivity to DM decays that yield observable photon lines. Our analysis covers the Galactic flux from DM decays in our halo and the extragalactic emission accumulated over all cosmic redshifts.

II. DARK MATTER DECAY FORMALISM

A. Halo decays: Dark matter rest frame

In natural units with $\hbar = c = 1$, the terrestrial photon flux from Galactic DM decays can be written as [2]

$$\frac{d\phi}{dE_\gamma} = \frac{1}{4\pi m\tau} \frac{dN_\gamma}{dE_\gamma} \int_{\Delta\Omega} d\Omega \int_{\text{los}} ds\, \rho(r), \qquad (1)$$

where m is the DM mass, τ is its lifetime, dN_γ/dE_γ is the differential photon flux per decay event, $d\Omega = d\ell\, db \cos b$ is the solid angle in terms of Galactic latitude b and longitude ℓ, $\Delta\Omega$ is the instrumental field of view, ρ is the DM density profile, and

$$r^2 = r_\odot^2 + s^2 - 2r_\odot s \cos b \cos \ell \qquad (2)$$

is the distance to the Galactic center (GC), $r_\odot = 8.25$ kpc is the solar distance from the GC, and s is the line of sight coordinate. We can also compactly write Eq. (1) as

$$\frac{d\phi}{dE_\gamma} = \frac{r_\odot \rho_\odot}{4\pi m\tau} \frac{dN_\gamma}{dE_\gamma} D, \qquad (3)$$

where the dimensionless D factor is

$$D \equiv \int_{\Delta\Omega} d\Omega \int_{\text{los}} \frac{ds}{r_\odot} \frac{\rho(r)}{\rho_\odot}, \qquad (4)$$

and we have integrated over the field of view.

To calculate the D factor, we model the DM density using a Navarro-Frenk-White (NFW) profile [9],

$$\rho(r) = \frac{\rho_0}{(r/r_s)(1 + r/r_s)^2}, \qquad (5)$$

where $r_s = 11$ kpc is the scale radius [10].[1] To assess the sensitivity of our results to the choice of the halo profile, we also consider the Einasto profile [11],

$$\rho(r) = \rho_0 \exp\left[-(r/r_s)^a\right], \qquad (6)$$

where $a = 0.91$ and $r_s = 3.86$ kpc is the scale radius [12]. For both profiles, the normalization parameter ρ_0 is chosen to recover the local DM density $\rho_\odot = 0.43$ GeV cm^{-3} [10].

Our signal of interest consists of a narrow x-ray line arising from a two-body DM decay process $\chi \to \gamma f$, where f is any particle. In both cases, the final state photons emerge nearly monochromatically with $E_\gamma = m/2$ in the rest frame of the decaying particle,

$$\left(\frac{dN_\gamma}{dE_\gamma}\right)_{\text{rest}} = \delta\left(E_\gamma - \frac{m}{2}\right), \qquad (7)$$

where δ is the Dirac delta function and we append an overall factor of 2 for the case where $f = \gamma$ and two photons are produced per decay.

B. Halo decays: Observer frame

As noted in Ref. [13], for instruments with fine grained energy resolution, the DM line signal is affected by Doppler broadening due to two effects; the DM velocity dispersion and the line-of-sight solar velocity with respect to the Galactic reference frame. Since LEM is projected to have unprecedented ~ 2 eV energy resolution, the energy deposited in the detector will be spread across several bins and the nature of the smearing depends on both the Galactic coordinates of the decay event and the velocity of the observer.

To account for the effect of DM velocity smearing, we first perform a thermal average in Eq. (1) taking the observer to be at rest with respect to the Galaxy,

$$\left(\frac{d\phi}{dE_\gamma}\right)_{\text{gal}} = \frac{1}{4\pi m\tau} \int_{\Delta\Omega} d\Omega \int_{\text{los}} ds\, \rho(r) \int du\, f_{\text{gal}}(u) \frac{dN_\gamma}{dE_\gamma}, \qquad (8)$$

where $u \equiv \vec{v} \cdot \hat{n}$ is the DM velocity $\vec{v}$ projected onto the line-of-sight unit vector,

$$\hat{n} = (\cos b \cos \ell, \cos b \sin \ell, \sin b), \qquad (9)$$

so the energy distribution is now Doppler shifted in the galaxy frame,

$$\frac{dN_\gamma}{dE_\gamma} = \delta\left(E_\gamma - \frac{m}{2}(1 + u)\right). \qquad (10)$$

In the Galactic rest frame, the line-of-sight velocity distribution can be written as

$$f_{\text{gal}}(u) = \frac{1}{\sqrt{\pi} v_0} e^{-u^2/v_0^2}, \qquad (11)$$

where we assume a constant velocity dispersion $v_0 \approx 220$ km/s.[2] Performing the u integration from Eq. (8) in the galaxy frame with the delta function from Eq. (10) yields to the thermally averaged energy distribution,

---

[1]Note that to improve the numerical stability of our D-factor integration, we remove the innermost region of the Galactic center between $r = 0$ and $r = 10^{-4}$ kpc, where the NFW profile is sharply peaked, so our results should be regarded as conservative.

[2]As found in Ref. [13], line broadening effects in the keV range are insensitive to the spatial dependence of v_0, so we adopt the constant local value throughout. Note also that the Doppler smearing in our treatment is barely resolvable, so our results are robust to variations with respect to the standard halo model used here.

$$g_{\text{gal}}(E_\gamma) \equiv \int du\, f_{\text{gal}}(u) \frac{dN_\gamma}{dE_\gamma}$$

$$= \frac{2}{\sqrt{\pi}mv_0} \exp\left[-\frac{4}{m^2 v_0^2}\left(E_\gamma - \frac{m}{2}\right)^2\right], \quad (12)$$

where the observer velocity is $\vec{v}_\odot = (0, v_\odot, 0)$ with $v_\odot = 220$ km/s, and there is implicit (b, ℓ) dependence from $\hat{n}$ in Eq. (9).

Finally, to account for the additional Doppler shift from the observer's velocity, the photon energy distribution becomes

$$g_{\text{obs}}(E_\gamma) = g_{\text{gal}}[E_\gamma(1 + \vec{v}_\odot \cdot \hat{n})], \quad (13)$$

and the flux in the observer frame is now

$$\left(\frac{d\phi}{dE_\gamma}\right)_{\text{obs}} = \frac{1}{4\pi m\tau} \int_{\Delta\Omega} d\Omega \int_{\text{los}} ds\, \rho(r) g_{\text{obs}}(E_\gamma), \quad (14)$$

which we integrate over our energy range of interest to compute the DM decay signal.

C. Extragalactic dark matter decay flux

The flux contribution from extragalactic DM decays integrated over all redshifts can be written as [14]

$$\left(\frac{d\phi}{dE_\gamma}\right)_{\text{eg}} = \frac{\Omega_{\text{dm}}\rho_c}{2\pi H_0 m^2 \tau} \sqrt{\frac{2E_\gamma}{m}} \frac{\Delta\Omega}{\sqrt{\Omega_m + \Omega_\Lambda (2E_\gamma/m)^3}}, \quad (15)$$

where $H_0 = 67.66$ km s^{-1} Mpc^{-1} is the present day Hubble constant, $\rho_c = 4.83 \times 10^{-6}$ GeV cm^{-3} is the critical density, $\Omega_i \equiv \rho_i/\rho_c$, $\Omega_{\text{dm}} = 0.2587$ is the fractional DM density, $\Omega_m = 0.3111$ is the fractional matter density, and $\Omega_\Lambda = 1 - \Omega_m \approx 0.68$ is the dark energy density [15].

III. BACKGROUND MODEL

In order to calculate the LEM sensitivity to DM x-ray decays, we need to estimate the background emission from Galactic and extragalactic sources in the instrumental field of view. In particular, the soft x-ray background is dominated by the Milky Way interstellar medium and by the cosmic x-ray background (CXB) [16]. The former is dominated by the emission from the hot gas, while the latter is mainly associated to distant active galactic nuclei [17]. The brightest Galactic emission lines in the energy range of interest are the O VII triplet, the Lyman alpha lines of O VIII and the faint Fe XVII [6,16].

Our emission model taken from Ref. [18] is shown in Fig. 1 (left panel) contains x-ray spectra computed from the Local Hot Bubble and Hot Halo [16]. The Local Hot Bubble is modeled using an unabsorbed APEC model [19] with temperature $T \approx 0.1$ keV. The Hot Halo component is modeled with two absorbed APEC components with

$T = 0.225$ keV and $T = 0.7$ keV. Note that the existence of the hotter component of the Hot Halo model is suggested by HaloSat observations [20]. The emission from the CXB follows the description from Ref. [21] which can be approximated with an absorbed power law with slope 1.47, whose normalization is calculated assuming half of the CXB sources are removed.[3] Note that different components dominates in different energy ranges. In particular, the diffuse Galactic and the local thermal-like emissions dominate below 1 keV, while the CXB dominates above 1 keV [22,23].[4]

In addition to the Milky Way and CXB, we also add a constant detector background rate of 1 event s^{-1} keV^{-1} [18], which corresponds to an additional $N_{\text{bg,det}} = 4 \times 10^4$ counts in each 2 eV bin, assuming a 20 Ms observation time. This contribution is not shown in Fig. 1, but is included in our background estimates and is subdominant to other backgrounds for all energies below ∼1 keV.

IV. RESULTS

To evaluate the LEM sensitivity to DM decays, we consider the following test statistic:

$$\chi^2(m, \tau) = \sum_{i=1}^{N_{\text{bin}}} \left(\frac{N_{\text{sig}}^i}{\sigma_i}\right)^2, \quad (16)$$

where the sum runs over the number of energy bins N_{bin} and the theoretical counts expected from DM in the ith bin are

$$N_{\text{sig}}^i = t_{\text{obs}} \int_{E_i}^{E_{i+1}} dE_\gamma A_{\text{eff}}(E_\gamma) \frac{d\phi}{dE_\gamma}(E_\gamma), \quad (17)$$

where $t_{\text{obs}} = 20$ Ms is the LEM observation time, A_{eff} is the corresponding effective area taken from Ref. [6], the bin size is 2 eV, and we separately calculate LEM projections using the flux from Eq. (14) for the Galactic contribution and Eq. (15) for the extragalactic contribution.

The conservative scenario corresponds to assuming that all detected lines arise from DM decays. In the realistic scenario we include the presence of emission lines due to the circumgalactic medium and intergalactic medium (the diffuse gas surrounding and between galaxies). The distribution of events observed by a telescope can be modeled

---

[3]In [6], the authors used the relation logN-logS of CXB sources (where N is the number counts and S represents the flux) to calculate that the bright end of the CXB sources corresponds to 50% of the total CXB flux and excluding these bright sources will result in loosing 2–3% of the LEM FOV.

[4]Reference [22] estimates the flux uncertainties for the Galactic and local thermal-like emissions to be of order 7%, while the CXB has an uncertainty in the flux of 13%. Note that Ref. [22] also shows that the statistical uncertainties dominate over the systematics ones.
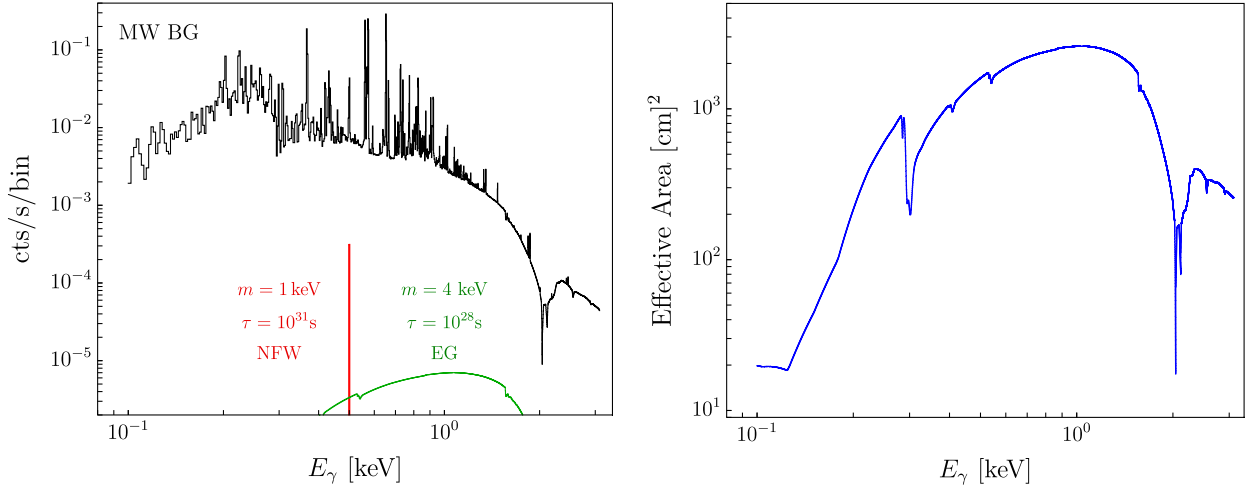
FIG. 1.   Left: Background of x-ray emission, which includes both Milky Way emission and contributions from the Cosmic x-ray background, which is mainly due to extragalactic active galactic nuclei. This emission is convolved with the effective area with 2 eV bins to generate the curve shown here (black histograms). Also shown are two narrow signal curves corresponding to representative benchmark points for Galactic decays with an NFW profile (red) and extragalactic (green) emission near the exclusion region shown in Fig. 2. Right: Projected effective area of the LEM telescope used in our analysis taken from Ref. [6].

with a binomial distribution. The standard deviation in each energy bin σ_i for a Poisson distribution is $\sqrt{N_{bg}^i}$, where N_{bg}^i includes the background count in the ith bin taken from Fig. 1 (scaled up by 20 Ms observing time) and the constant $N_{bg,det}$ detector background mentioned above. For each DM mass, this χ^2 has one degree of freedom, so to obtain LEM projections for the decay lifetime, we perform the Pearson's chi squared test and require $\chi^2 = 4(25)$ for 2σ exclusion (5σ discovery) sensitivity. Our main result is presented in Fig. 2 in the τ vs m plane assuming two x-rays are produced per DM decay from the Galactic Center ($b = \ell = 0°$).

In the left panel of Fig. 3 we interpret our projections from Fig. 2 in the context of an axionlike particle a that decays via $a \to \gamma\gamma$. The lifetime in this scenario can be written as [24]

$$\tau = \frac{64\pi}{g_{a\gamma\gamma}^2 m_a^3} \sim 10^{30} \text{ s} \left(\frac{10^{-17} \text{ GeV}^{-1}}{g_{a\gamma\gamma}}\right)^2 \left(\frac{\text{keV}}{m_a}\right)^3, \quad (18)$$

where $g_{a\gamma\gamma}$ is the diphoton coupling. Similarly, in the right panel, we interpret our results in the context of a sterile neutrino ν_s which can decay into active species via $\nu_s \to \nu\gamma$, yielding a single x-ray per decay event. The sterile neutrino radiative width to photon lines is [26]

$$\Gamma_\gamma = \frac{9\alpha G_F^2 \sin^2(2\theta) m_{\nu_s}^5}{1024\pi^4} \sim 10^{-32} \text{ s}^{-1} \left(\frac{\sin^2(2\theta)}{10^{-10}}\right) \left(\frac{m_{\nu_s}}{\text{keV}}\right)^5,$$
$$(19)$$

where α is the fine-structure constant, G_F is the Fermi constant, θ is the mixing angle and the lifetime satisfies

$\tau^{-1} = \Gamma_\gamma / \text{Br}(\nu_s \to \nu\gamma)$. Note that for sterile neutrinos below $m_{\nu_s} \lesssim 164$ eV [27], Tremaine-Gunn bound [28] excludes identical fermions from being all of the DM. Furthermore, if sterile neutrinos are produced through their interactions with Standard Model particles in the early Universe, there are also model-dependent limits from structure formation that exclude $m_{\nu_s} \lesssim$ few keV (e.g., [29]),
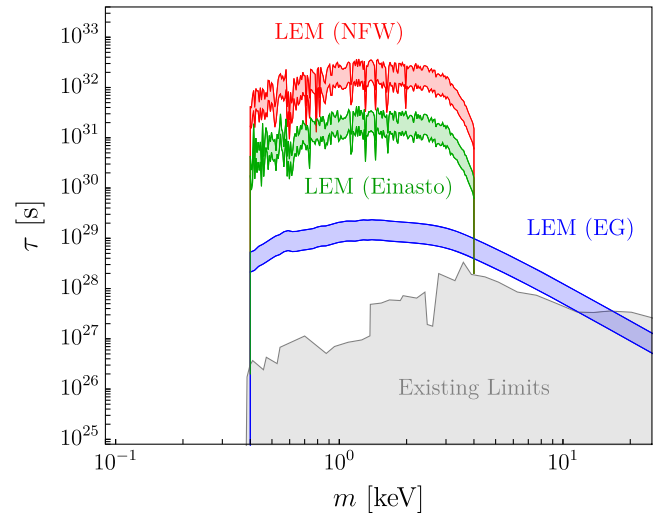

FIG. 2.   Projection for LEM sensitivity to DM diphoton decays in the lifetime vs mass plane. Here we use the effective area from Ref. [6], assuming an exposure time of 20 Ms. The red band shows the LEM 2–5σ sensitivity range assuming only decays from the Galaxy with an NFW profile, by looking at the Galactic Center. The green band shows the same result with an Einasto profile, and the blue band shows the corresponding projections for the extragalactic contribution. Also shown are existing limits on the DM mass and lifetime assuming diphoton decays [24,25].
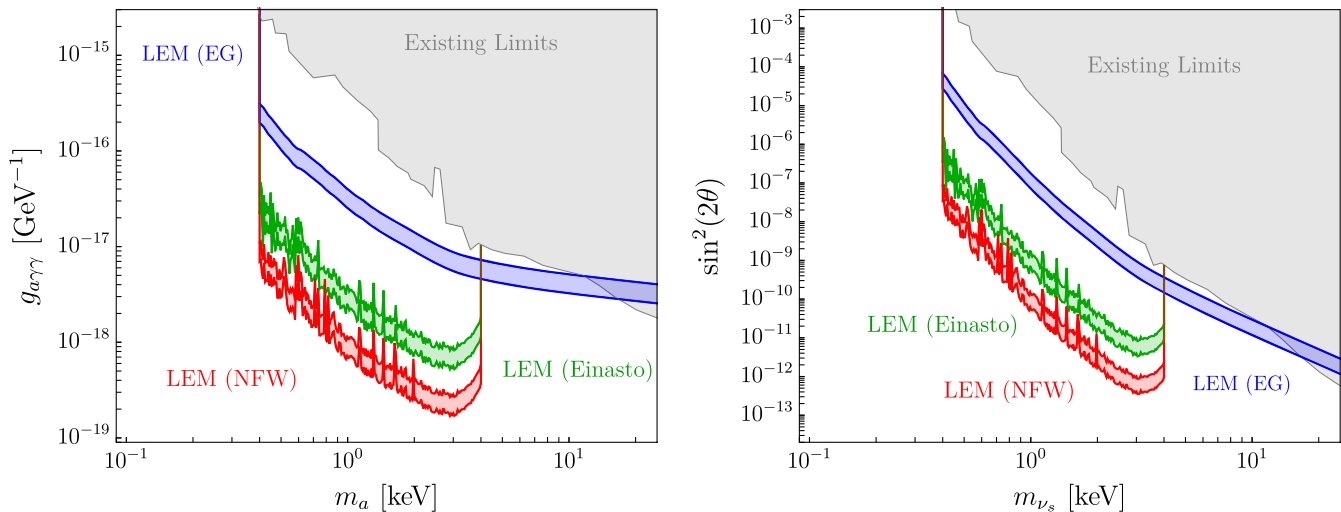
FIG. 3.   Left: Same analysis as in Fig. 2, but interpreted as a limit on the diphoton coupling $g_{a\gamma\gamma}$ of an axionlike particle a of mass m_a with lifetime given in Eq. (18) and existing limits taken from Refs. [24,25]. Right: Same constraints as the left panel, but interpreted as limits on sterile neutrino dark matter with mixing angle θ and mass m_{ν_s} with lifetime from Eq. (19).

which vary based on cosmological history and sterile neutrino production mechanisms. The main source of uncertainties is the background model. Following the measurements of the Micro-X Microcalorimeter x-Ray Sounding Rocket [30], at present day the x-ray background uncertainty is estimated to be a factor 5 in the photon counts,[5] which translated into an uncertainty of $\sqrt{5}$ in the DM bounds.

V. SUMMARY

In this work, we have demonstrated that the LEM telescope can greatly improve the sensitivity to DM photon line decays. We find that, due to the instrument's large grasp and high spectral resolution, a suitable survey can probe lifetimes of order $\sim 10^{32}$ s, exceeding current limits by four orders of magnitude in the few 100 eV–few keV mass range with an observation time of order 10 Ms.

---

[5]In 2018 the Micro-X Microcalorimeter x-Ray Sounding Rocket had its first flight. Figure 27 in Ref. [30] shows the data collected on its first flight with the respective uncertainties.

Since no instrument has ever been sensitive to DM lifetimes above $\sim 10^{30}$ s in any decay channel, LEM is poised to explore the longest DM lifetimes ever probed. In light of these promising results, LEM may also have sensitivity to secondary x-rays from DM decay and annihilation to charged particles, which we leave for future work.

[1] G. Bertone and D. Hooper, Rev. Mod. Phys. **90,** 045002 (2018).

[2] D. Hooper, Proc. Sci. TASI2018 (**2019**) 010 [arXiv:1812.02029].

[3] B. R. Safdi, Proc. Sci. TASI2022 (**2024**) 009 [arXiv:2303.02169].

[4] C. B. Adams et al., arXiv:2203.14923.

[5] K. N. Abazajian, Phys. Rep. **711–712,** 1 (2017).

[6] R. Kraft et al., arXiv:2211.09827.

[7] M. S. T. t. X. team, in Proceedings of the 16th Marcel Grossmann Meeting on Recent Developments in Theoretical and Experimental General Relativity, Astrophysics and Relativistic Field Theories (2023), 10.1142/9789811269776_0006.

[8] S. Das, K. Murase, and T. Fujii, Phys. Rev. D **107,** 103013 (2023).

[9] J. F. Navarro, C. S. Frenk, and S. D. M. White, Astrophys. J. **490,** 493 (1997).

[10] E. Karukes, M. Benito, F. Iocco, R. Trotta, and A. Geringer-Sameth, J. Cosmol. Astropart. Phys. (2019) 046.

[11] J. Einasto, Trudy Inst. Astrofiz. Alma-Ata **5,** 87 (1965).

[12] X. Ou, A.-C. Eilers, L. Necib, and A. Frebel, Mon. Not. R. Astron. Soc. **528,** 693 (2024).

[13] C. Dessert, O. Ning, N. L. Rodd, and B. R. Safdi, arXiv:2305.17160.

[14] R. Essig, E. Kuflik, S. D. McDermott, T. Volansky, and K. M. Zurek, J. High Energy Phys. 11 (2013) 193.

[15] N. Aghanim *et al.* (Planck Collaboration), Astron. Astrophys. **641,** A6 (2020); **652,** C4(E) (2021).

[16] D. McCammon, R. Almy, E. Apodaca, W. Bergmann Tiest, W. Cui, S. Deiker, M. Galeazzi, M. Juda, A. Lesser, T. Mihara, J. P. Morgenthaler, W. T. Sanders, J. Zhang, E. Figueroa-Feliciano, R. L. Kelley, S. H. Moseley, R. F. Mushotzky, F. S. Porter, C. K. Stahle, and A. E. Szymkowiak, Astrophys. J. **576,** 188 (2002).

[17] R. F. Mushotzky, L. L. Cowie, A. J. Barger, and K. A. Arnaud, Nature (London) **404,** 459 (2000).

[18] A. Bogdan *et al.*, Astrophys. J. **953,** 42 (2023).

[19] R. K. Smith, N. S. Brickhouse, D. A. Liedahl, and J. C. Raymond, Astrophys. J. **556,** L91 (2001).

[20] J. Bluem, P. Kaaret, K. Kuntz, K. Jahoda, D. Koutroumpa, E. Hodges-Kluck, D. LaRocca, and R. Ringuette, in *AAS/High Energy Astrophysics Division* (2022), Vol. 54, p. 400.02.

[21] R. C. Hickox and M. Markevitch, Astrophys. J. **645,** 95 (2006).

[22] R. C. Hickox and M. Markevitch, Astrophys. J. **645,** 95 (2006).

[23] C. Zhang *et al.*, arXiv:2310.02225.

[24] D. Cadamuro and J. Redondo, J. Cosmol. Astropart. Phys. 02 (2012) 032.

[25] C. O'Hare, cajohare/axionlimits: Axionlimits, https://cajohare.github.io/AxionLimits/ (2020).

[26] A. Palazzo, D. Cumberbatch, A. Slosar, and J. Silk, Phys. Rev. D **76,** 103511 (2007).

[27] A. Boyarsky, O. Ruchayskiy, and D. Iakubovskyi, J. Cosmol. Astropart. Phys. 03 (2009) 005.

[28] S. Tremaine and J. E. Gunn, Phys. Rev. Lett. **42,** 407 (1979).

[29] E. O. Nadler *et al.* (DES Collaboration), Phys. Rev. Lett. **126,** 091101 (2021).

[30] J. S. Adams *et al.* (Micro-X Collaboration), J. Astron. Telesc. Instrum. Syst. **9,** 034001 (2023).